Journal of Arrhythmia 33 (2017) 92–98

Contents lists available at ScienceDirect

Journal of Arrhythmia

journal homepage: www.elsevier.com/locate/joa

Original Article

The utility of atrial pacing for identifying the electrical breakthrough sites between the left atrium and pulmonary veins

Shinya Sugiura, MD[a,*], Koji Matsuoka, MD[a], Hideki Noda, BHS[a], Naoya Kurata, BHS[a], Misa Uemori, BHS[a], Hirokazu Shioji, MD[a], Akihiro Takasaki, MD[a], Takafumi Koji, MD[a], Takashi Tanigawa, MD[a], Masaaki Ito, MD[b]

[a] Department of Cardiology, Matsusaka Chuo Hospital, 102 KawaimachiKobou, Matsusaka, Mie 515-8566, Japan
[b] Department of Cardiology and Nephrology, Mie University Graduate School of Medicine, 2-174 Edobashi, Tsu, Mie 514-8507, Japan

ARTICLE INFO

Article history:
Received 28 April 2016
Received in revised form
26 July 2016
Accepted 8 August 2016
Available online 19 September 2016

Keywords:
Atrial fibrillation
Catheter ablation
Electrical breakthrough sites
Circumferential pulmonary vein isolation

ABSTRACT

Background: Circumferential pulmonary vein (PV) isolation for atrial fibrillation (AF) is occasionally difficult to achieve because electrical breakthrough sites (EBSs) between the left atrium (LA) and PVs cannot be identified during ablation especially in the carina regions.
Methods: The left PVs (Lt.PVs) of 60 AF patients and the right PVs (Rt.PVs) of 37 patients undergoing PV isolation were studied. When PV isolation was not achieved after the initial circumferential PV isolation, atrial pacing was repeatedly performed from the distal coronary sinus (CSd) and high right atrium (HRA), and the time interval from the stimulus to the earliest PV potential (stimulus-PV interval) was measured using circular mapping catheters at each PV until PV isolation was achieved. When PV isolation was achieved via local Radiofrequency (RF) deliveries, those regions were diagnosed as final EBSs. We classified the final EBSs into six segments for each PV (anterior and posterior PV walls of the roof, carina, and bottom) and investigated the relationship between the final EBSs and stimulus-PV intervals.
Results: For Lt.PVs, the stimulus-PV intervals during CSd pacing were significantly shorter than during HRA pacing at the Lt.PV anterior carina and bottom (90 ± 28 ms vs. 125 ± 26 ms, $P < 0.001$ and 84 ± 20 ms vs. 148 ± 24 ms, $P = 0.028$, respectively), but there was no significant difference in the Lt.PV roof and any posterior segments. For Rt.PVs, the stimulus-PV interval from both pacing sites exhibited no significant difference between either segment.
Conclusions: This pacing method may help to identify whether EBSs are located in the anterior Lt.PVs. Improved recognition of EBSs through pacing from different sites would be helpful for achieving PV isolation.

1. Introduction

Circumferential pulmonary vein (PV) isolation has been accepted by a consensus as the strategy for the treatment of atrial fibrillation (AF) using catheter ablation [1–4]. However, in some cases, it is difficult to achieve circumferential PV isolation because the electrical breakthrough sites between the left atrium (LA) and PVs during ablation cannot be identified, especially in the carina regions of each PV even though two circular mapping catheters are used and mapping of the earliest PV potentials is performed.

A few reports have demonstrated how to detect the electrical breakthrough sites between the LA and PVs [5,6]. However, there is no easy and useful method for achieving this. The objective of this study was to investigate the utility of atrial pacing for identifying the electrical breakthrough sites between the LA and PVs, especially in the carina regions of each PV.

2. Materials and methods

2.1. Study population

A total of 102 patients (31 women, 71 men, 63 ± 12 years) with drug-refractory, paroxysmal, or persistent AF who underwent circumferential PV isolation from January 2014 to March 2015 were enrolled. AF was classified according to the HRS/EHRA/ECAS 2012 Consensus Statement on the Catheter and Surgical Ablation of AF [7]. All patients gave their written informed consent and the study protocol was approved by the hospital's institutional review board.

* Corresponding author. Fax: +81 59 821 9555.
E-mail address: urasugi30@gmail.com (S. Sugiura).

http://dx.doi.org/10.1016/j.joa.2016.08.004

In this study, when PV isolation was not achieved after the initial circumferential PV ablation, to detect the electrical breakthrough sites between the LA and PVs, we repeatedly performed pacing from two different sites; the distal portion of the coronary sinus (CSd) and high right atrium (HRA), and measured the time interval from the stimulus to the earliest PV potential (stimulus-PV interval) on the circular mapping catheters at each PV until PV isolation was achieved. Therefore, we excluded patients with the following findings: (i) AF was sustained during catheter ablation even after electrical cardioversion was performed, (ii) the coronary sinus catheter could not be inserted into the vicinity of the left atrial appendage (LAA), (iii) PV isolation could be achieved after the initial circumferential PV ablation, and (iv) the atrium could not be captured by CSd or HRA stimulation. Consequently, the left PVs (Lt.PVs) of 60 patients and the right PVs (Rt.PVs) of 37 patients were investigated in this study.

2.2. Electrophysiological studies and catheter ablation

Antiarrhythmic drugs (AADs) were discontinued at least 5 half-lives prior to the procedure for paroxysmal AF but were continued for persistent AF. All patients were effectively anticoagulated with warfarin or non-vitamin K antagonist oral anticoagulants (NOACs) for at least 1 month before the procedure, and therapeutic anticoagulation was maintained with intravenous heparin following the discontinuation of NOACs 2 days prior to the procedure. Warfarin was continued during the perioperative period. Transesophageal echocardiography was performed within 24 h before the procedure to exclude any atrial thrombi. Cardiac enhanced computed tomography was performed for the evaluation of the relevant cardiac anatomy before the procedure.

The surface and intracardiac electrocardiograms were digitally recorded and stored (Lab System TM PRO EP Recording System, Bard Clearsign™, Boston Scientific Corporation). The bipolar electrograms were filtered from 30 to 500 Hz. A 6-Fr 20-pole three-site mapping catheter (BeeAT, Japan Lifeline, Tokyo, Japan) was passed through the right jugular vein for pacing, recording, and internal cardioversion. The four proximal electrodes, eight middle electrodes, and eight distal electrodes were in the HRA as close as possible to the sinus node, lateral right atrium, and CSd as close as possible to the LAA, respectively, throughout the procedure. The LA was accessed via a patent foramen ovale, when present, or via a transseptal puncture (through an 8-F long sheath; SL0, AF Division, St. Jude Medical, Minneapolis, MN, USA). Before the transseptal puncture, 3000 IU of heparin was administered and 5000 IU of heparin was administered after the transseptal puncture. Heparin was additionally administered to maintain the activated clotting time at 300–350 s. Two circular mapping catheters (Lasso, Biosense Webster, Inc. or Libero, Japan-Lifeline) were placed in the superior and inferior PVs, and the left- and right-sided ipsilateral PV ostia; and the left- and right-sided ipsilateral PVs were circumferentially and extensively ablated guided by a 3-D mapping system (CARTO3 system; Biosense-Webster). When AF occurred before or during the ablation, sinus rhythm was recovered using electrical cardioversion. The electrophysiological endpoint of the PV isolation was the achievement of a bidirectional conduction block between the LA and PVs. Radiofrequency catheter ablation was performed point-by-point using an open irrigated catheter (ThermoCool Smarttouch, Biosense-Webster) with the power and temperature limited to 20–35 W and 43 °C, respectively. The esophageal temperature was measured (using Sensitherm, St. Jude Medical or Esophaster, Japan-Lifeline) during the applications to avoid any esophagus-related complications [8–10], and the Radiofrequency (RF) energy delivery was stopped if the esophageal temperature reached 40 °C. After completing the PV isolation, a 20–40 mg bolus of adenosine triphosphate and 5–20 μg/min of

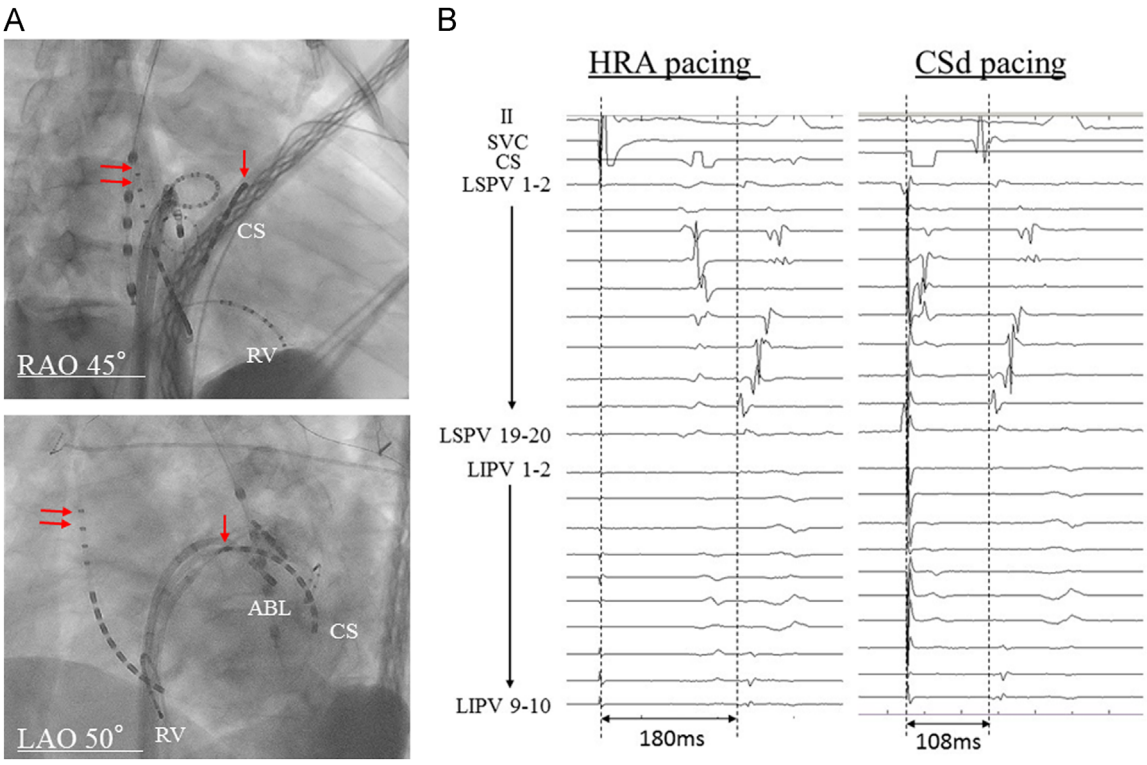

Fig. 1. (A) Fluoroscopic images of the left pulmonary vein (PV) during ablation. Two circular mapping catheters were placed in the ipsilateral left PVs. Pacing was performed from the distal coronary sinus (CSd; arrow) and high right atrium (HRA; two arrows). The ablation catheter (ABL) was placed at the successful site in the anterior region of the LIPV. (B) Intracardiac recordings during HRA pacing and CSd pacing in the same case as (A). The stimulus-PV interval during CSd pacing was shorter than that during HRA pacing (108 ms vs. 180 ms). *LAO* left anterior oblique; *RAO* right anterior oblique; *CS* coronary sinus; *RV* right ventricular; *ABL* ablation catheter; *LSPV* left superior pulmonary vein; *LIPV* left inferior pulmonary vein, *SVC* superior vena cava.

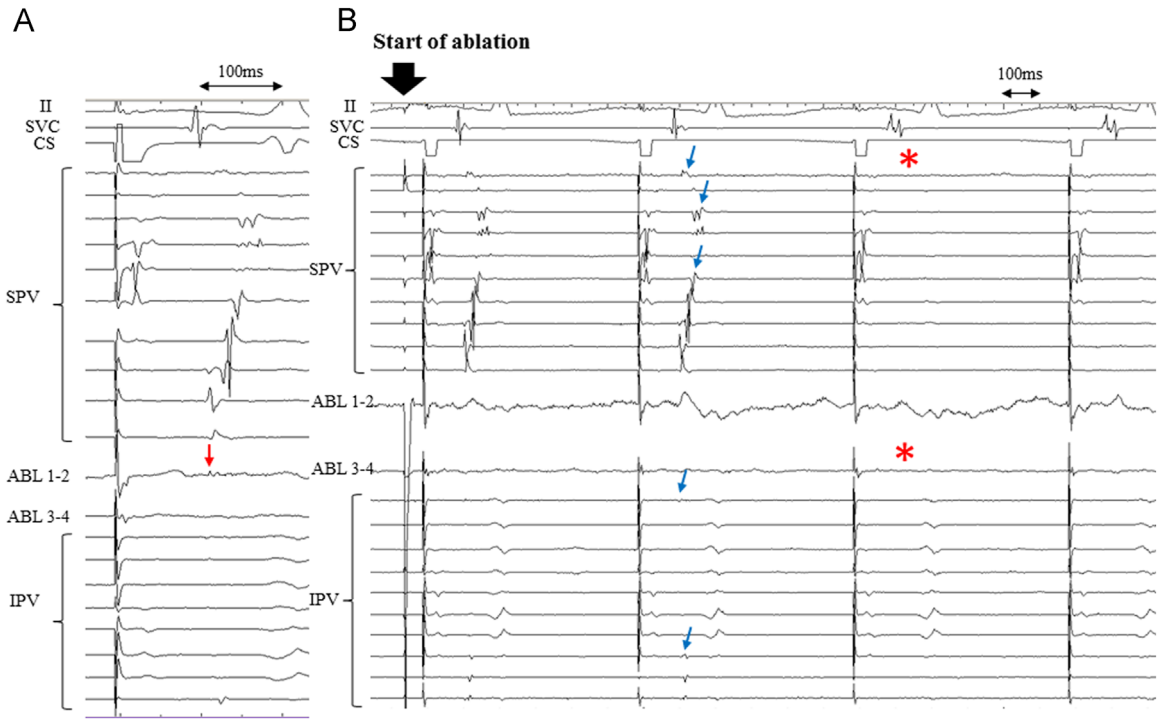

Fig. 2. Intracardiac recordings during the successful ablation in the same case as Fig. 1A. (A) The earliest fragmented low amplitude potential (red arrow) was observed on the ABL in the anterior region of the left IPV. (B) The ipsilateral left PVs (blue arrows) were simultaneously isolated from the LA by RF applications at this site (asterisk). *CS* coronary sinus; *ABL* ablation catheter; *SPV* superior pulmonary vein; *IPV* inferior pulmonary vein; *SVC* superior vena cava.

Table 1
The clinical characteristics of the patients regarding the left and right pulmonary veins (PVs).

	Left PVs (n=60)	Right PVs (n=37)
Age (years)	62 ± 12	59 ± 13
BMI (kg/m^2)	25 ± 4	25 ± 4
Male/Female	41/19	28/9
BNP (pg/ml)	82 ± 85	73 ± 96
LAD (mm)	45 ± 8	44 ± 11
LVEF (%)	68 ± 9	79 ± 9
Structural heart disease, n (%)	13 (22)	8 (22)
Hypertension, n (%)	36 (60)	20 (54)
Diabetes mellitus, n (%)	9 (15)	4 (11)
Stroke/TIA, n (%)	8 (13)	5 (14)
Vascular disease, n (%)	10 (17)	5 (14)
$CHADS_2$ score	1 ± 1	1 ± 1
CHA_2DS_2-VASc score	2 ± 2	2 ± 2
Persitent AF, n (%)	32 (53)	20 (54)
AADs, n (%)	27 (45)	14 (38)
Re-Ablation, n (%)	7 (12)	6 (16)
After Rt. PV isolation, n (%)	15 (25)	8 (22)

BNP brain natriuretic peptide; *LAD* left atrial dimension; *LVEF* left ventricular ejection fraction; *TIA* transient ischemic attack; *$CHADS_2$* congestive heart failure, hypertension, age ≥75, diabetes, stroke (doubled); *CHA_2DS_2-VASc* congestive heart failure, hypertension, age ≥75 (doubled), diabetes, stroke (doubled), vascular disease, age 65–74 years, and female sex; *AF* atrial fibrillation; *AADs* antiarrhythmic drugs; *After Rt. PV isolation* a left PV isolation was performed after the right PV isolation was achieved.

isoproterenol were injected to unmask any dormant PV conduction [11], and any gaps responsible for dormant conduction were eliminated using additional RF applications.

2.3. Measurement of the time interval from the pacing stimulus to the earliest PV potential on the circular mapping catheters

When circumferential PV isolation was not achieved after the initial circumferential PV ablation, to identify the electrical breakthrough sites between the LA and PVs, we performed pacing with a cycle length of 600 ms from two different sites: (i) CSd as the vicinity of the LAA, and (ii) HRA as the vicinity of the sinus node (Fig. 1A). Subsequently, we measured the stimulus-PV interval on the circular mapping catheters at each PV (Fig. 1B). When circumferential PV isolation was not achieved even after additional RF current was delivered, we repeatedly performed the above pacing procedure and measured the above time interval until PV isolation was achieved. When the circumferential PV isolation was eventually achieved using localized RF delivery, we diagnosed that region as the final electrical breakthrough site (Fig. 2).

After the PV isolation, we classified the final breakthrough sites into six anatomic segments of each PV (anterior and posterior PV walls of the roof, carina, and bottom) and investigated the relationship between the final electrical breakthrough sites and stimulus-PV intervals by pacing from the CSd and HRA.

2.4. Statistical analysis

SPSS statistical software package (version 19.0J, SPSS Japan Inc., an IBM company) was used for all statistical calculations. Data were expressed as the mean ± SD. Comparisons between groups were performed with the Student's t-test. Qualitative parameters were compared using chi-square analysis or Fisher's exact test. P-values of <0.05 were considered statistically significant.

3. Results

3.1. Patient characteristics

Isolation of Lt.PVs in 42 patients (41%) and Rt.PVs in 65 patients (64%) was achieved after the initial circumferential PV ablation. A large number of patients were apparently excluded from the Rt.PV group. As a result, the Lt.PVs in 60 patients and Rt.PVs in 37 patients were investigated in this study.

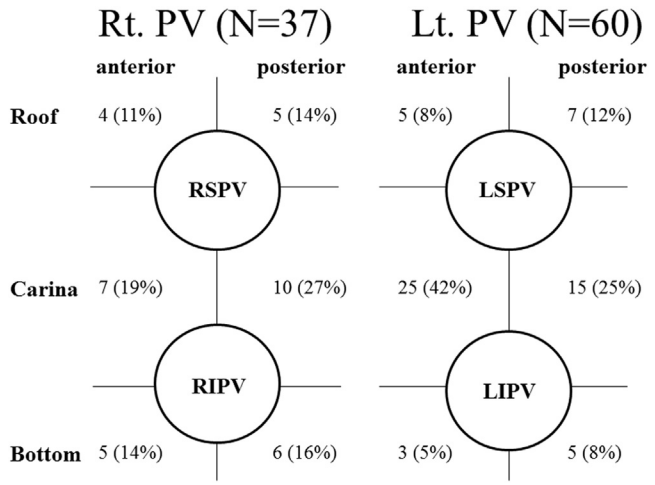

Fig. 3. Prevalence of electrical breakthrough sites in the anatomic segments of each pulmonary vein (PV). Each breakthrough site was classified into six segments around the ostium of the PV (anterior and posterior walls of the roof, carina, and bottom of the PVs). The numbers described around each PV perimeter represent the prevalence of breakthrough sites in these six segments (100% means that a breakthrough was observed in that segments on each side of the PVs). *LSPV* left superior pulmonary vein; *LIPV* left inferior pulmonary vein; *RSPV* right superior pulmonary vein; *RIPV* right inferior pulmonary vein.

The stimulus-PV intervals were measured at the Lt.PVs of 60 patients and Rt. PVs of 37 patients by pacing from the CSd and HRA. The clinical characteristics of the patients for each PV are shown in Table 1.

For the Lt.PVs, we identified 60 patients (62 ± 12 years) with nonvalvular AF (NVAF) (including 36 patients with persistent AF). In 15 patients (25%), a Lt.PV isolation was performed after the Rt.PV isolation was achieved. Seven patients (12%) underwent a second AF ablation session. AADs were used with pilsicainide in 2 patients, flecainide in 1, amiodarone in 2, and bepridil in 22. For the Rt.PVs, we identified 37 patients (59 ± 13 years) with NVAF (including 20 patients with persistent AF). AADs were used with amiodarone in 1 patient and bepridil in 13.

3.2. Comparison of the patients for the six anatomic segments of each PV

The final electrical breakthrough sites were classified into six segments (anterior roof, anterior carina, anterior bottom, posterior roof, posterior carina, and posterior bottom) for each PV. The prevalence of breakthrough sites in the six anatomic segments of each PV is shown in Fig. 3. For the Lt.PVs, the highest prevalence (25%) of breakthrough sites was at the anterior carina. However, for the Rt.PVs, the highest prevalence (10%) of breakthrough sites was at the posterior carina. The stimulus-PV intervals during CSd and HRA pacing are shown in Table 2. For the Lt.PVs, the stimulus-PV intervals during CSd pacing were significantly shorter than those during HRA pacing for the anterior Lt.PVs (92 ± 27 ms vs. 126 ± 30 ms, $P < 0.001$), but there was no significant difference between the two pacing sites for the posterior Lt.PVs (115 ± 36 ms vs. 118 ± 37 ms, $P = 0.616$). For the Rt.PVs, the stimulus-PV interval from both pacing sites exhibited a significant difference for both the anterior and posterior regions. Furthermore, at the anterior carina and bottom of the Lt.PVs, the stimulus-PV intervals during CSd pacing were significantly shorter than during HRA pacing (90 ± 28 ms vs. 125 ± 26 ms, $P < 0.001$, 84 ± 20 ms vs. 148 ± 24 ms, $P = 0.028$, respectively). However, for the anterior roof of the Lt.PVs, there was no significant difference between the two pacing sites (105 ± 25 ms vs. 116 ± 18 ms, $P = 0.536$). In regard to the posterior region of all segments of the Lt.PVs, there was no significant difference in the stimulus-PV interval during either CSd or HRA pacing. Howbeit, for the Rt.PVs, there was no significant difference between the two pacing sites for each segment. Based on the receiver operating characteristic curve for the difference in the stimulus-PV interval between the two pacing sites for the anterior carina and bottom of the Lt.PVs, the most effective cutoff difference for the stimulus-PV interval between the segments was 9.5 ms. The degree of sensitivity was 92.9% and the specificity was 70.0% (Fig. 4).

4. Discussion

The present study demonstrates that HRA and CSd pacing might aid the improved recognition of the electrical breakthrough sites, especially in the anterior region of the carina of the Lt.PVs during ablation. Howbeit, this pacing method was not useful for identifying breakthrough sites at the roof and posterior regions of the Lt.PVs and all regions of the Rt.PVs.

Table 2
Comparison of the stimulus-PV interval during HRA and CSd pacing for each PV.

Final breakthrough site	Stimulus-PV interval during HRA pacing (ms)	Stimulus-PV interval during CSd pacing (ms)	*P* value
Anterior Left. PV ($N=33$)	126 ± 30	92 ± 27	< 0.001
Posterior Left. PV ($N=27$)	118 ± 37	115 ± 36	0.616
Anterior Right. PV ($N=16$)	93 ± 26	121 ± 27	0.001
Posterior Right. PV ($N=21$)	85 ± 30	103 ± 25	0.004

Comparison of the stimulus-PV interval during HRA and CSd pacing from six segments of the left. PVs

Final breakthrough site	Stimulus-PV interval during HRA pacing (ms)	Stimulus-PV interval during CSd pacing (ms)	*P* value
Anterior Roof ($N=5$)	116 ± 18	105 ± 25	0.536
Posterior Roof ($N=7$)	114 ± 44	123 ± 43	0.164
Anterior Carina ($N=25$)	125 ± 26	90 ± 28	< 0.001
Posterior Carina ($N=15$)	118 ± 31	113 ± 39	0.577
Anterior Bottom ($N=3$)	148 ± 24	84 ± 20	0.028
Posterior Bottom ($N=5$)	126 ± 51	109 ± 16	0.578

PV pulmonary vein; *HRA* high right atrium; *CSd* distal coronary sinus.

Recognizing the electrical breakthrough sites between the LA and PVs is essential for reaching the endpoint of the circumferential PV isolation. However, in some cases, it is not easy to recognize these breakthrough sites especially in the anterior and posterior regions of the carina of each PV even though two circular mapping catheters are used and mapping to find the earliest PV potential is performed. Some reasons for this are that the ablation line is far from the position of these mapping catheters and the architecture of the myocardial sleeves between that line and these catheters varies and is complex [12–14]. A few reports have demonstrated how to detect the electrical breakthrough sites between the LA and PVs. However, to the best of our knowledge, no simple and useful method for detecting these breakthrough sites has been reported. In this study, we measured the stimulus-PV interval during CSd and HRA pacing and investigated whether or not the electrical breakthrough sites could be identified, especially in the carina regions of each PV.

This time interval between two components depended on how long each pacing stimulus took to activate the myocardium of each PV. The direction of the myocardial activation wavefront towards each PV differed between pacing from the CSd and HRA. During pacing from the CSd, the myocardium of the LAA was activated first. Subsequently, the activation wavefront immediately proceeded towards the Lt.PVs via an anterior site of the Lt.PVs, which was adjacent to the LAA [15,16]. Consequently, it took a shorter time to activate the myocardium of the Lt.PVs. Further, the Rt.PVs were activated late because they were the furthest from the CSd in the LA. Hence, it took a longer time to activate the myocardium of the Rt.PVs. However, during pacing from the HRA, the myocardium of the RA was activated first and the activation wavefront proceeded to an anterior and roof site on the right side of the LA through Bachmann's bundle, and the Rt.PVs were activated early [17]. In addition, the Lt.PVs were activated late because the Lt.PVs were the furthest from the HRA in the LA. Thus, it took a longer

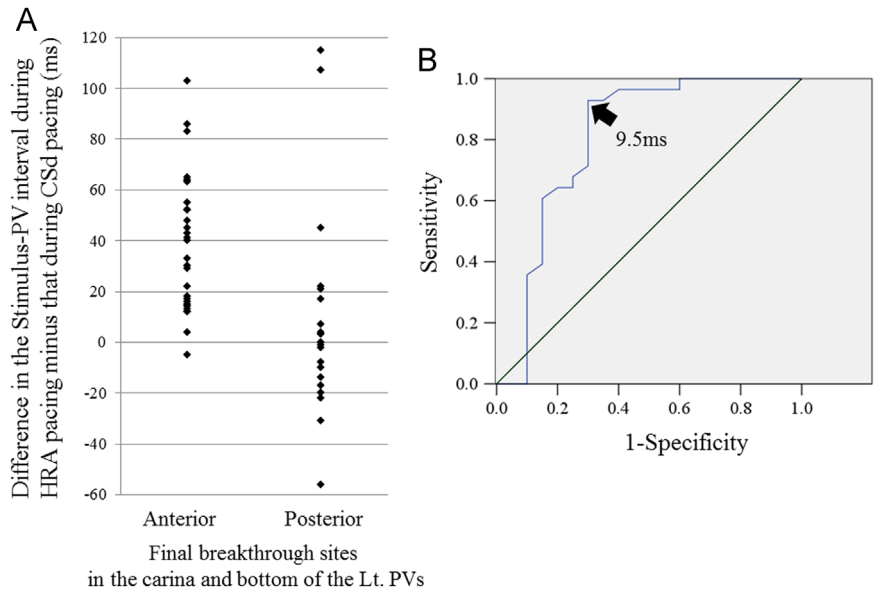

Fig. 4. (A) Distribution of the difference in the stimulus-PV interval during HRA pacing minus that during CSd pacing. (B) Calculation of the optimal cutoff value using a receiver operating characteristic curve analysis with respect to the difference in the stimulus-PV interval during HRA pacing minus that during CSd pacing. A receiver operating characteristic analysis yielded an optimal cutoff value of 9.5 ms. The area under the receiver operating characteristic curve was 0.804 (95% CI 0.658–0.950, $P < 0.001$). *CSd* distal coronary sinus; *HRA* high right atrium.

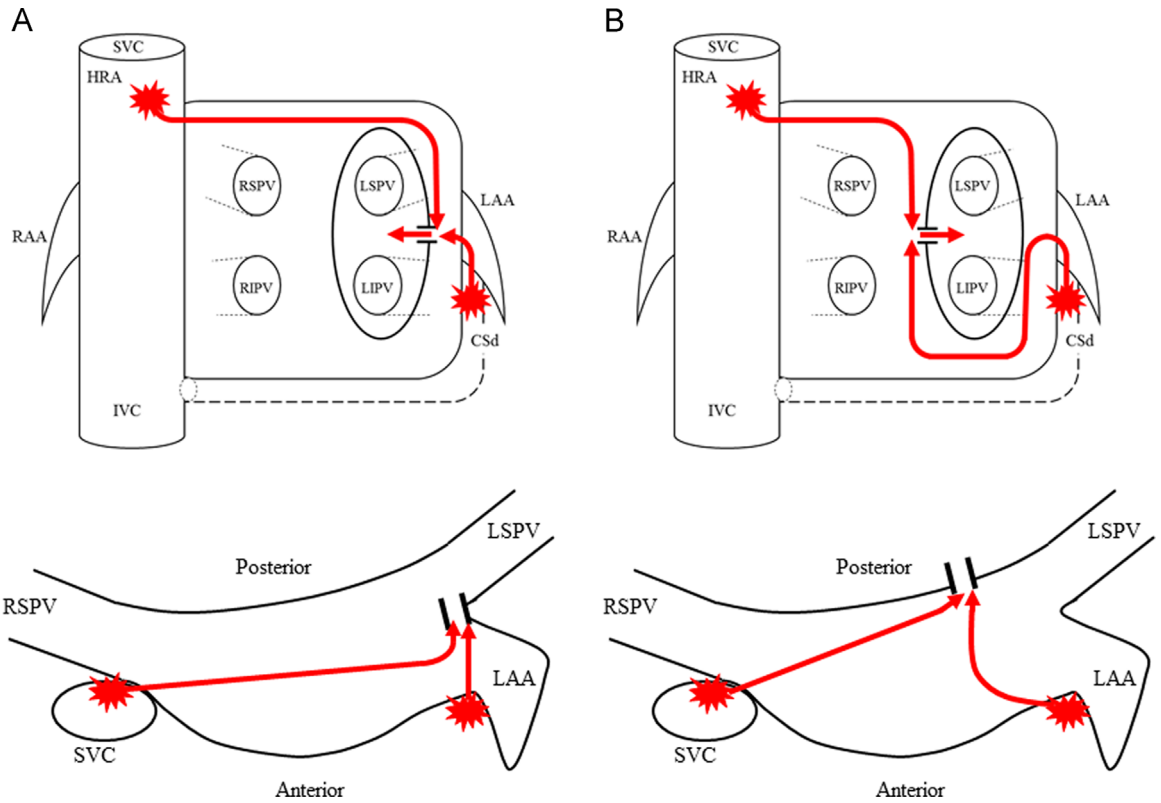

Fig. 5. The activation wavefront at each electrical breakthrough site in the left pulmonary veins (PVs). (A) A case with an electrical breakthrough site in the anterior region of the left PVs. The upper and lower diagrams are schemas in the coronal and axial view, respectively, from the roof of the atrium. (B) A case with an electrical breakthrough site in the posterior region of the left PVs. The upper and lower diagrams are schemas in the coronal and axial view, respectively, from the roof of the atrium.

time to activate the myocardium of the Lt.PVs, and in cases with electrical breakthrough sites in the anterior carina and bottom of the Lt.PVs, the stimulus-PV interval during CSd pacing was significantly shorter than that during HRA pacing (Fig. 5A). Further, in cases with connections between the LA and roof or posterior segments of the Lt.PVs, which meant that the electrical breakthrough sites did not occur in the anterior carina of the Lt.PVs, the activation wavefront moving towards the Lt.PVs proceeded through a posterior site because the wavefront could no longer immediately proceed through an anterior site of the Lt.PVs, and

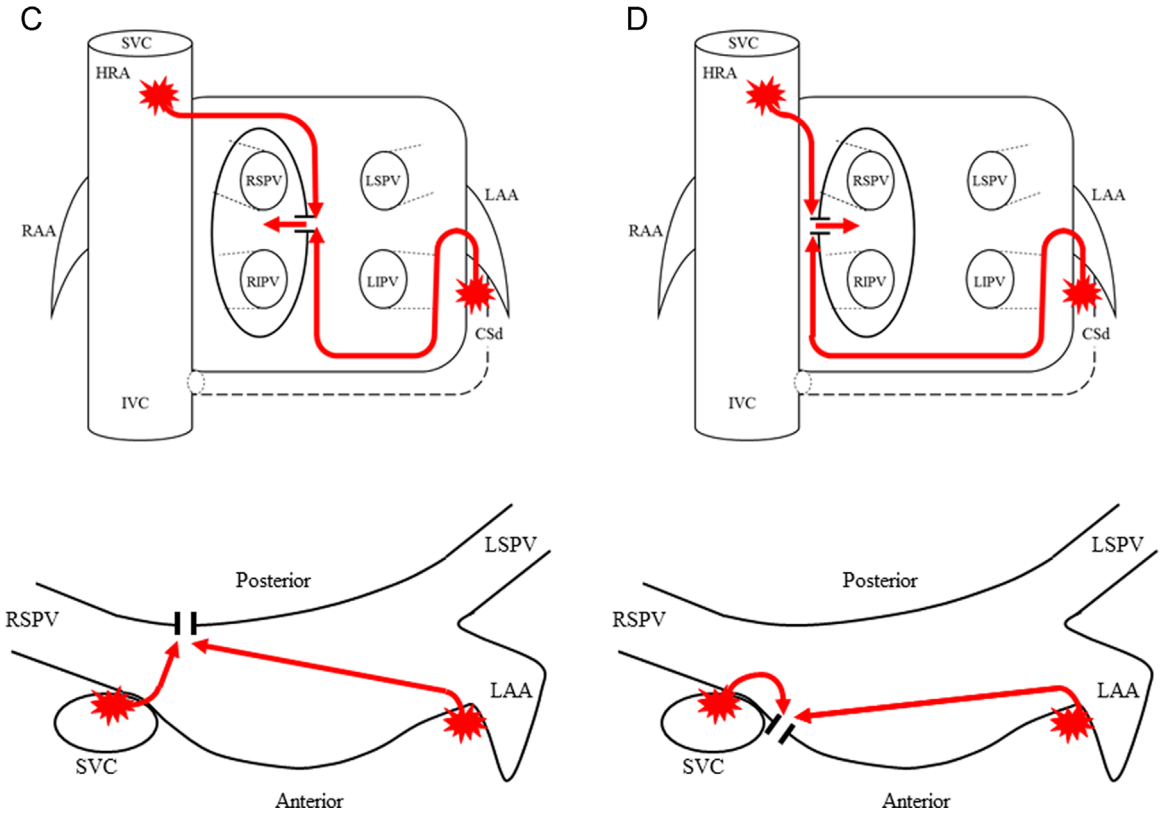

Fig. 6. The activation wavefront at each electrical breakthrough site in the right pulmonary veins (PVs). (C) A case with an electrical breakthrough site in the posterior region of the right PVs. The upper and lower diagrams are schemas in the coronal and axial view, respectively, from the roof of the atrium. (D) A case with an electrical breakthrough site in the anterior region of the right PVs. The upper and lower diagrams are schemas in the coronal and axial view, respectively, from the roof of the atrium.

accordingly, it took a longer time to activate the Lt.PVs. Consequently, there was no significant difference in the stimulus-PV interval during either CSd or HRA pacing (Fig. 5B).

Equally, in regards to the Rt.PVs, because there was a significant difference in the direction of the myocardial activation wavefront between that during CSd and that during HRA pacing, there was a significant difference in the time it took to activate the PVs (Fig. 6C, D). However, in this study, this pacing method was not useful for discriminating the breakthrough sites for the Rt.PVs. It is necessary, in the future, to establish how to identify the breakthroughs sites especially in the carina region of the Rt.PVs.

When PV isolation was not achieved after the initial and/or repeated circumferential PV isolation, detailed mapping of gaps along the PVI isolation line was often performed. Nevertheless, in some cases, it might not have been easy to record visible PV potentials in those ablation regions because the amount of myocardium might have been diminished to a greater or lesser extent by the burn of the ablation application and edema may have been induced. These findings were recognized especially in the anterior carina of the Lt.PVs although the ablation catheter was appropriately placed at the breakthrough site during ablation. For such cases, we recommend that our pacing method might be helpful for the improved recognition of the electrical breakthroughs during the ablation. Although our method did not accurately lead to the detection of the breakthrough point in all PVs, it was relatively easier to identify whether or not the electrical breakthrough sites between the LA and carina were from the region of the Lt.PVs. Consequently, this pacing method may help to minimize ineffective radiofrequency deliveries, complications [8–10,18], hard labor, procedure time, and provide a better ablation outcome.

4.1. Limitation

First, this study was a single-center endeavor and a relatively small sample of patients was included. Second, in this study, our method could not strictly lead to the detection of the breakthrough point in all PVs. Therefore, to make our method more effective in clarifying the breakthrough sites in all PVs, pacing from other sites such as sites proximal to the coronary sinus or the posterior region of the LA should be considered. In addition, our pacing method was not useful for identifying the electrical breakthrough sites when multiple electrical breakthrough sites existed. However, our method could aid in determining whether there are breakthrough sites in the anterior region of the left PVs. Third, the distance from these pacing sites to each PV varies from patient to patient. In addition, the position and configuration of the CSd, HRA, and each PV also vary from patient to patient. Furthermore, the difference in the stimulus-PV intervals between CSd pacing and HRA pacing may depend on the position of the PV isolation line. Therefore, the stimulus-PV interval may have been influenced by these factors in this study. Fourth, for the Lt.PVs, the results of the Lt.PV isolation were the same regardless of whether it was a first right PV isolation or a repeat ablation. However, for the Rt.PVs, the stimulus-PV interval may have been influenced by whether it was a first Rt.PV isolation or a repeat ablation. The results should be confirmed in larger patient groups.

5. Conclusions

We suggest that the pacing method described in this study is helpful in ascertaining whether the electrical breakthrough sites are located at an anterior left PV site. Improved recognition of the

electrical breakthrough sites by pacing from different sites would be helpful for achieving a PV isolation.

Conflict of interest

All authors declare no conflicts of interest related to this study.

Acknowledgments

We would like to express our thanks to Mr. John Martin for his assistance in the preparation of this manuscript.

References

[1] Natale A, Raviele A, Arentz T, et al. Venice Chart international consensus document on atrial fibrillation. J Cardiovasc Electrophysiol 2007;18:560–80.
[2] Haïssaguerre M, Jaïs P, Shah DC, et al. Electrophysiological end point for the catheter ablation of atrial fibrillation initiated from multiple pulmonary venous foci. Circulation 2000;101:1409–17.
[3] Haïssaguerre M, Jaïs P, Shah DC, et al. Spontaneous initiation of atrial fibrillation by ectopic beats originating in the pulmonary veins. N Engl J Med 1998;339:659–66.
[4] JCS Joint Working Group. Guidelines for non-pharmacotherapy of cardiac arrhythmias (JCS 2011): Digest version. Circ J 2013;77:249–74.
[5] Yamane T, Shah DC, Jaïs P, et al. Electrogram polarity reversal as an additional indicator of breakthroughs from the left atrium to the pulmonary veins. J Am Coll Cardiol 2002;39:1337–44.
[6] Arentz T, von Rosenthal J, Blum T, et al. Feasibility and safety of pulmonary vein isolation using a new mapping and navigation system in patients with refractory atrial fibrillation. Circulation 2003;108:2484–90.
[7] Calkins H, Kuck KH, Cappato R, et al. 2012 h/EHRA/ECAS Expert Consensus Statement on Catheter and Surgical Ablation of Atrial Fibrillation: recommendations for patient selection, procedural techniques, patient management and follow-up, definitions, endpoints, and research trial design. Europace 2012;14(4):528–606.
[8] Cappato R, Calkins H, Chen SA, et al. Prevalence and causes of fatal outcome in catheter ablation of atrial fibrillation. J Am Coll Cardiol 2009;53:1798–803.
[9] Kuwahara T, Takahashi A, Takahashi Y, et al. Incidences of esophageal injury during esophageal temperature monitoring: a comparative study of a multi-thermocouple temperature probe and a deflectable temperature probe in atrial fibrillation ablation. J Interv Card Electrophysiol 2014;39:251–7.
[10] Kuwahara T, Takahashi A, Kobori A, et al. Safe and effective ablation of atrial fibrillation: importance of esophageal temperature monitoring to avoid peri-esophageal nerve injury as a complication of pulmonary vein isolation. J Cardiovasc Electrophysiol 2009;20:1–6.
[11] Hachiya H, Hirao K, Takahashi A, et al. Clinical implications of reconnection between the left atrium and isolated pulmonary veins provoked by adenosine triphosphate after extensive encircling pulmonary vein isolation. J Cardiovasc Electrophysiol 2007;18:392–8.
[12] Haïssaguerre M, Shah DC, Jaïs P, et al. Electrophysiological breakthroughs from the left atrium to the pulmonary vein. Circulation 2000;102:2463–5.
[13] Ho SY, Sanchez-Quintana D, Cabrera JA, et al. Anatomy of the left atrium: implications for radiofrequency ablation of atrial fibrillation. J Cardiovasc Electrophysiol 1999;10:1525–33.
[14] Saito T, Waki K, Becker AE. Left atrial myocardial extension onto pulmonary veins in humans: anatomic observations relevant for atrial arrhythmias. J Cardiovasc Electrophysiol 2000;11:888–94.
[15] Shah D. Electrophysiological evaluation of pulmonary vein isolation. Europace 2009;11:1423–33.
[16] Shah D, Haïssaguerre M, Jais P, et al. Left atrial appendage activity masquerading as pulmonary vein potentials. Circulation 2002;105:2821–5.
[17] Masuda R, Miyazaki S, Kusa S, et al. Discrimination of thoracic vein potentials facilitated by atrial pacing during the isolation. Pacing Clin Electrophysiol 2015;38:225–30.
[18] Robbins IM, Colvin EV, Doyle TP, et al. Pulmonary vein stenosis after catheter ablation of atrial fibrillation. Circulation 1998;98:1769–75.